

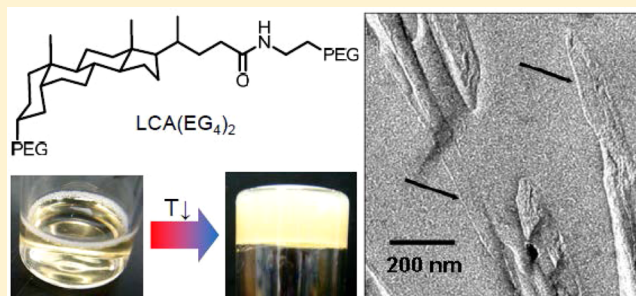
## Self-Assembly of Bile Acid–PEG Conjugates in Aqueous Solutions

Satu Strandman, Frantz Le Dévédec, and X. X. Zhu\*

Department of Chemistry, Université de Montréal, CP 6128, Succursale Centre-ville, Montreal, QC H3C 3J7, Canada

## Supporting Information

**ABSTRACT:** Thermoresponsive characteristics of oligo(ethylene glycol) derivatives of lithocholic acid (LCA) depend on the hydrophilic/hydrophobic balance of the compounds. Below a threshold temperature ( $\sim 30^\circ\text{C}$ ), one of the derivatives,  $\text{LCA}(\text{EG}_4)_2$ , self-assembles in water into hollow nanotubes that form thixotropic gels at high concentrations. Two concentration regimes were observed in the plateau moduli ( $G_0 \sim G'$ ). At high concentrations, the mobility of the nanotubes is restricted at the ordered microdomains acting as cross-links. In semidilute aqueous solutions, the linkers between the aggregated domains in the fragile gel rupture easily, and this effect depends strongly on dilution. Organic hydrophobic additives perturb the self-assembling process, leading to changes in the two transition temperatures and poorer mechanical properties of the gel.



## 1. INTRODUCTION

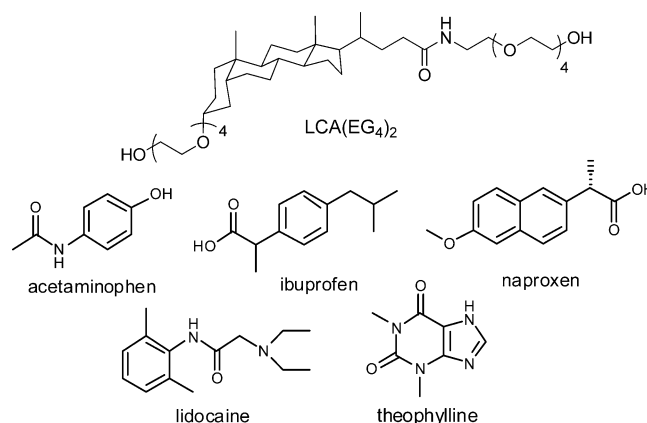
The aggregation of macromolecules and low-molar-mass compounds into elongated self-assemblies such as wormlike micelles, fibers, or tubules has been an interesting topic of research, as the directed self-assembly increases the viscosity of the solutions, often to the point of gelation. Such one-dimensional nanostructures are promising candidates for drug delivery vehicles providing long circulation times in body,<sup>1</sup> as packing materials for separation,<sup>2</sup> as templates for metal nanowires,<sup>3</sup> and as biocides<sup>4</sup> or in photo- or biocatalysis.<sup>5,6</sup> Some of the amphiphilic molecules capable of self-assembling into nanotube-like structures are diacetylenic phospholipids, peptides, glycolipids, and amphiphilic derivatives of polycyclic aromatic hydrocarbons, among others.<sup>7</sup> Another interesting group of compounds also capable of this type of self-organization are bile acids, which are endogenous steroids known to form gels at high concentrations and appropriate pH conditions.

The structure of bile acids predisposes them to a complex self-assembling behavior as the hydrophobic and hydrophilic domains are less separated than with other common surfactants.<sup>8</sup> These facially amphiphilic molecules show stepwise aggregation in water involving hydrophobic association of apolar faces of bent steroid backbones responsible for primary aggregation, followed by hydrogen-bonding interactions of the hydrophilic groups.<sup>9</sup> This leads to a directed self-assembly and gelation at high concentrations, which can be enhanced by tuning the pH of the solution or by derivatizing the carboxylic acid group with hydrogen bond-forming or charged moieties.<sup>10</sup> Some of the bile acid derivatives are also known as organogelators, forming gels in organic solvents.<sup>11,12</sup> The viscoelastic behavior depends strongly on the structure of the bile acid derivatives,<sup>10</sup> varying from soft viscoelastic solids to more complex systems resembling polyelectrolyte gels. The

hydrophilic groups of bile acids can also act as handles for building complex molecular and macromolecular architectures, such as molecular pockets<sup>13–15</sup> and umbrellas,<sup>16</sup> and star polymers.<sup>17,18</sup>

We have earlier reported the thermoresponsive characteristics of an amphiphilic oligo(ethylene glycol)-grafted lithocholate<sup>19</sup> that exhibits two thermal transitions in aqueous solutions in contrast to more densely grafted deoxycholate and cholate derivatives that show only one phase transition temperature, the cloud point. Upon cooling, a solution of the lithocholate derivative  $\text{LCA}(\text{EG}_4)_2$  (Scheme 1) becomes cloudy at  $\sim 30^\circ\text{C}$

**Scheme 1. Structures of the Lithocholate Derivative  $\text{LCA}(\text{EG}_4)_2$  and the Compounds Used in the Study as Organic Additives**



Received: August 10, 2012

Revised: October 29, 2012

Published: December 7, 2012

due to a phase transition, and the polarized optical micrographs of the sample below this temperature have suggested the presence of fibrillar species.<sup>19</sup> Here, oligo(ethylene glycol)s can be attached via anionic polymerization method as side arms onto lithocholic acid to make it soluble at physiological pH as well as for tuning the thermoresponsiveness and physical properties of its aqueous solutions. It is known that even small structural modifications of bile acids and their analogues may lead to completely different self-assembling characteristics and physical properties of aggregated samples.<sup>10</sup> In this paper, we present the viscoelastic properties and the gelation of LCA(EG<sub>4</sub>)<sub>2</sub> in aqueous solutions, visualize the self-assemblies responsible for gelation, and compare the results with those reported for bile acids and their other derivatives. The attempts to correlate the structural modifications with the self-assembling and gelation properties have sometimes led to unexpected results,<sup>10</sup> which warrants the studies on various types of steroid derivatives as potential gelators, including the structurally simple oligo(ethylene glycol)-grafted bile acids. In addition, to gain a better understanding on the self-assembling process in the presence of additives, we studied the effect of model compounds (drugs) with different polarities and hence different solubilities in water on the thermal transitions in view of potential applications in pharmaceutical field.

## 2. EXPERIMENTAL SECTION

**2.1. Materials.** Oligo(ethylene glycol) derivative of lithocholic acid, LCA(EG<sub>4</sub>)<sub>2</sub>, was synthesized according to a previously reported procedure<sup>17</sup> by anionic polymerization of ethylene oxide. The characterization of the derivative has been described earlier.<sup>19</sup> Number-average molar mass ( $M_n$ ) is 770 g mol<sup>-1</sup>, and the polydispersity index (PDI) is 1.02, as determined by MALDI-TOF mass spectrometry. Acetaminophen, ibuprofen, lidocaine, naproxen, and theophylline (Scheme 1) were purchased from Aldrich and used as received. The logarithm of octanol–water partition coefficient  $\log P$  is commonly used to describe the hydrophobicity of compounds and is defined as  $\log P = \log([c]_{\text{octanol}}/[c]_{\text{water}})$ , where  $[c]$  is the concentration of the studied compound in a selected solvent. The literature values of  $\log P$  for the model compounds are listed in Table 1.

**Table 1. Water Solubilities and Logarithmic Octanol–Water Partition Coefficients at 25 °C ( $\log P$ ) and  $pK_a$  Values<sup>46</sup> of Selected Model Compounds (Drugs) as Well as Mixing Temperatures ( $T_{\text{mix}}$ ) and Cloud Points ( $T_{\text{cp}}$ ) of 1.5 wt % Solutions of LCA(EG<sub>4</sub>)<sub>2</sub> Containing Drug at a Molar Ratio 0.4 (Estimated Error  $\pm 1$  °C)**

drug	water solubility (g L <sup>-1</sup> )	$\log P$	$pK_a$	$T_{\text{mix}}$ (°C)	$T_{\text{cp}}$ (°C)
acetaminophen	14	0.5	9.38	32	73
theophylline	7.4	0.0	8.81	33	68
lidocaine	4.1	2.4	8.01	28	66
ibuprofen	$21 \times 10^{-3}$	4.0	4.91	21	35
naproxen	$16 \times 10^{-3}$	3.2	4.15	24	33

**2.2. Methods.** Rheological measurements were performed with a TA Instruments AR2000 stress-controlled rheometer equipped with a Peltier plate for temperature control. A 40 mm 2° steel cone and a 60 mm 2° acrylic cone were used for the oscillatory measurements. The measuring setup was covered with a solvent trap to avoid evaporation of water from the

samples and the condensation of humidity on the setup cooled to 5 °C. The linear viscoelastic regime was established by oscillatory stress sweeps using stress range from  $5.97 \times 10^{-3}$  to 298 Pa. The samples were presheared for 10 s at a known stress (24 Pa) prior to the equilibration of 24 h to ensure identical handling conditions. The measurements were carried out at 5 °C, well below the gel-to-solution temperature of the samples. Oscillatory measurements were conducted at a constant frequency ( $f = 1$  Hz) and strain ( $\sigma = 0.1\%$ ) in the linear viscoelastic regime.

Freeze-fracturing and transmission electron microscopy (TEM) of aqueous solutions of the bile acid derivative were performed as described earlier.<sup>17</sup> The platinum–carbon replicas were imaged with FEI Tecnai 12 120 kV transmission electron microscope equipped with Gatan 792 Bioscan 1k × 1k wide-angle multiscan CCD camera.

Turbidimetric measurements of the aqueous solutions of LCA(EG<sub>4</sub>)<sub>2</sub> with the selected model compounds (drugs) were done on a Varian Cary 300 Bio UV–vis spectrophotometer. The samples were prepared by mixing a selected model compound with LCA(EG<sub>4</sub>)<sub>2</sub> in methanol, after which the solvent was removed by freeze-drying. The mixture was dissolved in water, followed by an equilibration overnight at 5 °C prior to the measurements. The pH values of the solutions were  $\sim 7$ . The heating rate was adjusted at 0.2 °C min<sup>-1</sup> and the detection wavelength was 400 nm. The LCA(EG<sub>4</sub>)<sub>2</sub> concentration was 1.5 wt %. Transmittances were normalized by  $T_{\text{norm}} = (T - T_{\text{min}})/(T_{\text{max}} - T_{\text{min}})$  and plotted as a function of temperature. The mixing temperature  $T_{\text{mix}}$  was defined as the point at which the transmittance reached the maximum, and the cloud point  $T_{\text{cp}}$  was determined from the point where transmittance decreased to 50%.

## 3. RESULTS AND DISCUSSION

**3.1. Solution Properties of the Lithocholic Acid Derivatives.** Lithocholic acid (LCA) is poorly water-soluble at the physiological pH or below it but can dissolve in alkaline solutions. Many linear and branched amphiphilic oligo-(ethylene glycol) derivatives, such as nonionic surfactants,<sup>20</sup> show phase separation upon heating and are often quite hydrophobic, resulting in lower cloud points than with PEGs. The pegylation of lithocholic acid yields a cloud point ( $T_{\text{cp}}$ ) observed at  $\sim 79$  °C for LCA(EG<sub>4</sub>)<sub>2</sub>. This transition depends on the steric hindrance of bile acid derivatives. For example, CA(EG<sub>2</sub>)<sub>4</sub> having the same total number of ethylene glycol units but a higher number of grafts, obtained by using cholic acid as a core instead of lithocholic acid, has a higher  $T_{\text{cp}}$  ( $>90$  °C).<sup>19</sup> In addition, the thermosensitivity of LCA derivatives is governed by a delicate hydrophobic/hydrophilic balance: a small increase in the length of grafts from 4 to 6 units (LCA(EG<sub>6</sub>)<sub>2</sub>,  $M_n = 1040$  g mol<sup>-1</sup>, PDI = 1.03) leads to an increase in the cloud point ( $>90$  °C) and a disappearance of the second phase transition (mixing temperature  $T_{\text{mix}}$ ) observed at  $\sim 29$ – $32$  °C for LCA(EG<sub>4</sub>)<sub>2</sub>. Further increase in the graft length to 9 units (LCA(EG<sub>9</sub>)<sub>2</sub>,  $M_n = 1330$  g mol<sup>-1</sup>, PDI = 1.04) increases the solubility, and no cloud point was observed below the boiling point of water.

Below the mixing temperature, LCA(EG<sub>4</sub>)<sub>2</sub> forms a cloudy gel at high concentrations ( $\geq 10$  wt %) that becomes transparent after several days of equilibration at 5 °C, indicating increased homogeneity of the sample with time. The gels were viscous enough to stay on the bottom of a tilted vial but become liquidlike when shaken, similar to the gels formed by

sodium lithocholate (NaLC) or deoxycholate (NaDC).<sup>9</sup> The gelation along with the dual thermoresponsive behavior has recently been described also for a PEG conjugate of betulin, a pentacyclic triterpene with facially amphiphilic characteristics in its conjugated form.<sup>21</sup> Figure 1 presents a TEM micrograph of a

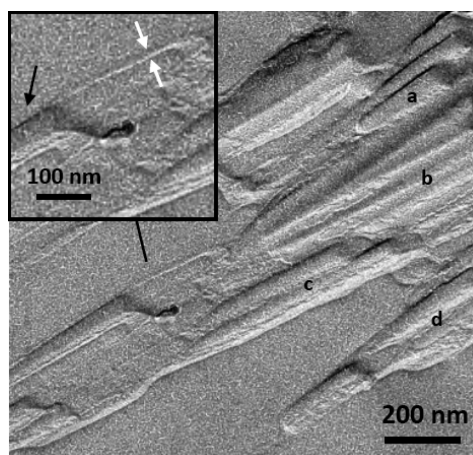


**Figure 1.** A representative TEM micrograph of a freeze-fractured carbon-platinum replica of 10.0 wt % LCA(EG<sub>4</sub>)<sub>2</sub> sample. The inset shows an expanded region of the micrograph, presenting a single nanotube-like self-assembled structure. The black arrow points to the outer surface, and white arrows point out a wall of a horizontally fractured tube. The letters a–d mark regions with bundled nanotubes.

replica of freeze-fractured 10 wt % LCA(EG<sub>4</sub>)<sub>2</sub> sample showing bundled rigid nanotubes (Figure 1a–d), aligned upon the shear of preparing the specimen. Although cryo-TEM has become more popular in imaging liquid or semiliquid samples, freeze-fracture TEM (FF-TEM) is a technique that has been used successfully for visualizing nanotubes or nanofibers in high-viscosity specimens in both aqueous and organic solutions, for example for lithocholic acid,<sup>22</sup> self-assembling diamides,<sup>23</sup> or peptides.<sup>24</sup> Similar to FF-TEM micrographs of peptide nanotubes shown in the literature,<sup>25,26</sup> horizontally fractured LCA(EG<sub>4</sub>)<sub>2</sub> nanotubes with visible walls can be observed together with intact tubes. The walls have been pointed out in the inset of the micrograph in Figure 1, and the interior has the same density as the exterior, indicating hollow structures. The uniform wall thickness measured from the micrographs is  $6.7 \pm 0.9$  nm, in accordance with the wide-angle X-ray scattering (WAXS) result of an equilibrated sample ( $6.3 \pm 0.9$  nm, data shown in Figure S1 of the Supporting Information). The diameter of the tubes is  $\sim 50$  nm, and the lengths can be several micrometers. However, estimating the diameters and the lengths is difficult due to the fracturing of the tubes at different depths.

The wall thickness of sodium lithocholate (NaLC) nanotubes reported by Terech and co-workers<sup>27</sup> is 3 nm, determined by small-angle X-ray scattering (SAXS). As the length of the lithocholic acid molecule  $L_{\text{LCA}}$  is 1.4 nm<sup>28</sup> (another literature value 1.65 nm<sup>29</sup>), such dimensions would suggest a lamellar structure of the nanotube wall, supported by the studies on the crystal structure of bile acids<sup>28</sup> and bile acid-based gelators<sup>30</sup> that form dimers through hydrogen bonding. In fact, the coexistence of single- and multilayered walls has been observed in the TEM micrographs of LCA<sup>22</sup> and peptide nanotubes,<sup>25</sup> although in the case LCA, the multilayers eventually disappeared after long equilibration. A coarse estimation of

the dimensions of LCA(EG<sub>4</sub>)<sub>2</sub> based on the  $L_{\text{LCA}}$  and the contour lengths of EG<sub>4</sub> grafts ( $L_c = 1.4$  nm, based on the monomer length  $0.358$  nm<sup>31</sup> at an all-trans conformation) would give a theoretical maximum length of the molecule  $L_{\text{max}} = 4.2$  nm. As this value is smaller than the observed wall thickness and the true dimensions of the molecule in aqueous solution are expected to be smaller than the theoretical ones, double-layer formation could be one possibility for the self-assembly of LCA(EG<sub>4</sub>)<sub>2</sub> into the nanotube walls, commonly observed for bolaform amphiphiles (bolaamphiphiles), which are compounds consisting of a hydrophobic skeleton bound between two hydrophilic moieties.<sup>32</sup>

**3.2. Viscoelastic Properties of the Solutions.** The equilibration of LCA(EG<sub>4</sub>)<sub>2</sub> gels after preshearing has been followed through the increase in storage and loss moduli,  $G'$  and  $G''$ , as a function of time (Figure 2a). For instance, a 17.0 wt % sample reached the equilibrium after  $\sim 20$  h. This kinetic evolution can be assigned to the growth of the elongated self-

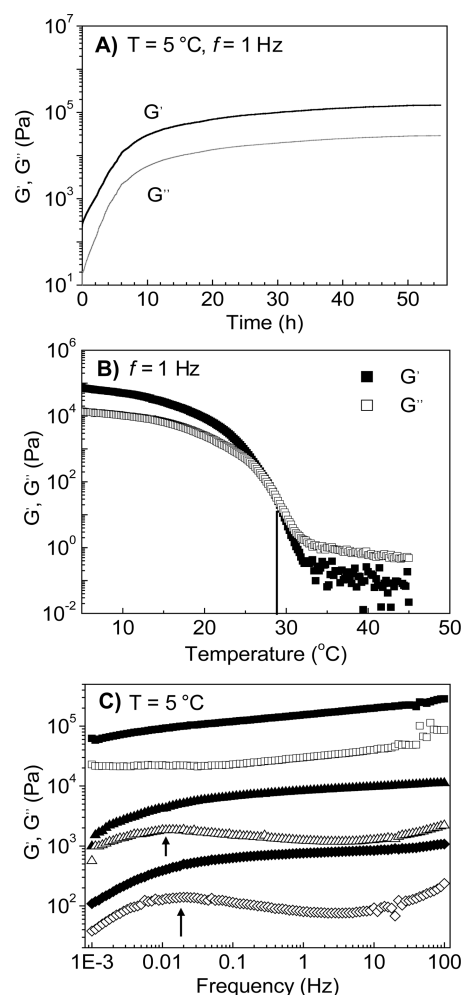


**Figure 2.** (A) Time evolution of storage modulus  $G'$  and loss modulus  $G''$  after preshearing and (B) oscillatory temperature sweep at a heating rate  $0.2$  °C  $\text{min}^{-1}$ , both for a 17.0 wt % sample of LCA(EG<sub>4</sub>)<sub>2</sub>. The gel-to-sol temperature,  $T = 28.6$  °C, is marked with a line (corresponding to the point where  $G' = G''$ ). (C) Mechanical spectra (oscillatory frequency sweeps) of LCA(EG<sub>4</sub>)<sub>2</sub> solutions, concentrations from top down: 17.0 wt % ( $G'$ , ■;  $G''$ , □), 7.5 wt % ( $G'$ , ▲;  $G''$ , △), and 5.0 wt % ( $G'$ , ◆;  $G''$ , ◇). The arrows point to the maxima in  $G''$  at the low-frequency range.



assemblies and their network formation, common for organo- and hydrogelators based on small organic compounds.<sup>33</sup> As mentioned above, neither a mixing temperature nor gelation was observed for the oligo(ethylene glycol) derivatives of deoxycholates or cholates, even when the grafts were as short as two repeating units, suggesting the critical role of steric hindrance and thus of molecular packing on the self-assembling process. The gel-to-sol transition of a 17.0 wt % gel takes place at 28.6 °C (Figure 2b), where  $G''$  exceeds  $G'$  upon heating at the oscillation frequency of 1 Hz. The result is in accordance with our earlier results on the mixing temperature of the aqueous  $\text{LCA}(\text{EG}_4)_2$  solutions by differential scanning calorimetry (DSC) and turbidimetry. The gel-to-sol transition temperature is lower than that of sodium lithocholate gels (61 °C)<sup>34</sup> owing to the higher water solubility of the oligo(ethylene glycol) derivative of lithocholate.

The mechanical spectra ( $G'$  and  $G''$  as a function of frequency) of  $\text{LCA}(\text{EG}_4)_2$  at different concentrations are shown in Figure 2c. The spectra exhibit the characteristics of weak gels with the slight frequency dependence of  $G'$  and  $G''$  that increases toward the higher dilution. The ratio  $G''/G'$  describing the strength of the gel is above 0.1 ( $\sim 0.3$ – $0.6$ ) throughout the studied concentration range 5.0–17.0 wt %, similar to the soft tissues and biological hydrogels, such as collagen and polysaccharide networks<sup>35</sup> as well as the self-assembled fibrillar networks of bile salt analogues.<sup>10</sup> The loss moduli at lower concentrations (5 and 7.5 wt %) show a broad bump referring to a distribution of slow relaxation modes with relaxation times  $\tau \sim 50$ – $90$  s, which are faster than those of the gels of tripod-shaped cholamides (also known as molecular pockets,  $\tau \sim 300$  s) reported in the literature.<sup>10</sup> This behavior was assigned to partially arrested dynamics of the rodlike self-assemblies,<sup>36</sup> more obvious at higher dilutions due to the higher mobility of the assemblies. Similar observations were also made for the hydrogels formed by nanotubes of lanthanum–cholate complexes.<sup>37</sup>

As an approximation,  $G'$  at a sufficiently high oscillatory frequency can be taken as the plateau modulus  $G_0$  used in the scaling relationships describing the nature of the network. Here, the values of  $G'$  at a frequency of 1 Hz are selected for comparison, and their concentration dependence is plotted in Figure 3. The samples display two regimes where the scaling of the  $G'$  is different. At a concentrated regime, the scaling exponent of  $\text{LCA}(\text{EG}_4)_2$  is 1.6, which is higher than that of sodium lithocholate gels (exponent 1.0)<sup>27,33</sup> but lower than those of several deoxycholate-based bile salt analogues

(exponents 2.0–2.8)<sup>33</sup> or small-molecule organogelators (exponents  $\sim 2.1$ ).<sup>38</sup> The theoretical scaling<sup>39</sup> of the concentration dependence is  $G' \sim C^{5/2}$  for densely cross-linked gels and  $G' \sim C^{11/5}$  for entangled solutions. The high scaling exponents of the gels of bile salt analogues have been explained by their behavior as energetic networks with a low degree of freedom in the fiber trajectories, while the low value of scaling exponent of NaLC gels indicates free rotation around the cross-linking nodes in the network.<sup>33</sup> For comparison, semiflexible networks of a filamentous bacteriophage<sup>40</sup> or microtubules<sup>41</sup> have shown the scaling exponent of 1.4. Cross-linking of the microtubules led to an increase in the exponent to 1.6–1.8, depending on the degree of cross-linking and, hence, the mobility of the tubules in the network.<sup>41</sup> Therefore, we may conclude that at the concentrated regime, the motion of  $\text{LCA}(\text{EG}_4)_2$  nanotubes around the connecting points is partially restricted. This may stem from the ordered microdomains acting as cross-links, formed through the bundling of nanotubes observed in the TEM micrographs. In addition to entangling, the fiber-like self-assemblies of various bile acid-based compounds can interact via mechanisms such as parallel merging, electrostatic-driven associations, or crystallization.<sup>10</sup>

Below a threshold concentration of  $\sim 9$  wt %, the scaling exponent is 7.5, and thus, the concentration dependence of  $G'$  is high, which is typical for a semidilute regime, reflecting the quickly increasing number of elastically active elements upon concentration. Terech and co-workers<sup>10</sup> have also observed two scaling regimes of  $G'$  for the aqueous solutions of a cationic *N*-methylmorpholine deoxycholate with scaling exponents of 2.8 (concentrated solutions) and 5.1 (semidilute solutions). The two scaling regimes have been explained through a scaling theory of colloidal gels,<sup>42</sup> where the theoretical structure of colloidal networks involves floc-like elements, further aggregating with each other to build a macroscopic gel. The relative strength of the interactions inside the flocs and between them differentiates the two major concentration regimes. At semidilute solutions and “weak-link regime”, intrafloc interactions prevail and the gels are typically fragile. At high concentrations and “strong-link regime”, interfloc interactions become dominant and determine the network elasticity. The two scaling regimes have also been described for the solutions of associative polymers, where the theoretical number of transient network junctions arising from intermolecular hydrophobic interactions is strongly concentration-dependent.<sup>43,44</sup> The high scaling exponent of  $\text{LCA}(\text{EG}_4)_2$  at the semidilute regime arises from the high mobility of  $\text{LCA}(\text{EG}_4)_2$  nanotubes, which promotes the disruption of the network upon dilution.

**3.3. Effect of Organic Additives.** One of the suggested applications of bile acid-based gels is topical drug delivery,<sup>45</sup> owing to their thixotropy and expected biocompatibility. Hence, our interest has been to investigate the effect of organic additives on the thermal transitions and viscoelastic properties of  $\text{LCA}(\text{EG}_4)_2$ . Previous reports have dealt with the effect of different salts and pH on the gelation of bile salts<sup>11</sup> as well as with the gelation of NaLC in alcohols such as methanol, ethanol, and ethylene glycol.<sup>29</sup> Polyols, such as mannitol and glycerol, commonly used in dermal and cosmetic formulations, have been shown to influence the viscosity of NaDC gels through hydrogen bonding.<sup>45</sup> In some cases, the cosolvents may improve the partition between the hydrophilic and hydrophobic domains, leading to a better stability of the gels.<sup>11</sup> We have earlier shown that added salt (NaCl) has no effect on the on the mixing transition ( $T_{\text{mix}}$ ) of  $\text{LCA}(\text{EG}_4)_2$ , but

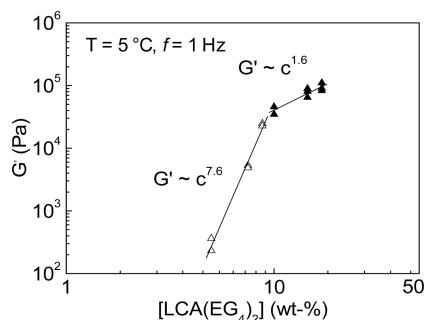


**Figure 3.** Scaling of the storage modulus  $G'$  with concentration. Different symbols (closed and open triangles) are used to emphasize the two scaling regimes. The lines correspond to the linear fits on the data.

it decreases the cloud point ( $T_{cp}$ ) through the salting-out effect on oligo(ethylene glycol) moieties.<sup>19</sup> This could indicate that hydrophobic interactions play an important role in the mixing transition assigned to the self-assembling process.

Therefore, we have selected some common drugs (Scheme 1) as model compounds representing different water solubilities and hydrophobicities (represented by logarithmic octanol–water partition coefficients,  $\log P$ ), all bearing both hydrogen bond donors and acceptors. The water solubilities of the compounds follow the order naproxen < ibuprofen < lidocaine < theophylline < acetaminophen (Table 1). This is the reverse order of their effect on the cloud point of LCA(EG<sub>4</sub>)<sub>2</sub>, shown in Figure 4a. While acetaminophen and theophylline decrease

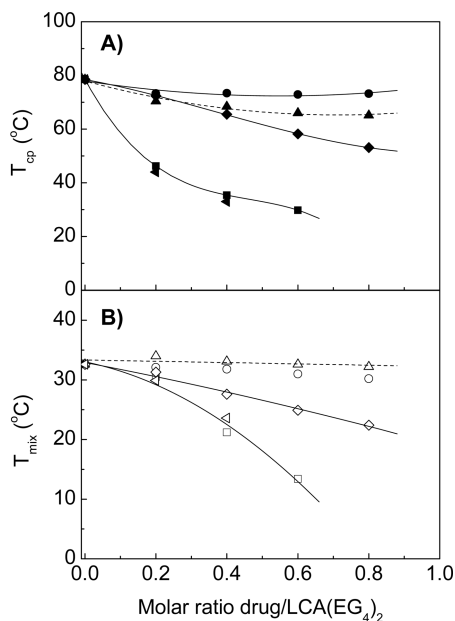


**Figure 4.** Effect of model compounds (drugs) ibuprofen (■, □), lidocaine (◆, ◇), theophylline (▲, △), naproxen (◄, ◄), and acetaminophen (●, ○) on (A) the cloud point ( $T_{cp}$ ) and (B) the mixing temperature ( $T_{mix}$ ) of 1.5 wt % LCA(EG<sub>4</sub>)<sub>2</sub> observed by UV–vis spectroscopy at detection wavelength of 400 nm and heating rate of 0.2 °C min<sup>−1</sup>. Estimated error of transition temperatures is  $\pm 1.0$  °C. Lines have been added as visual guides.

the cloud point of LCA(EG<sub>4</sub>)<sub>2</sub> slightly from  $\sim 79$  °C, a more significant decrease is observed for the less water-soluble drugs, ibuprofen and naproxen. Amphiphilic LCA(EG<sub>4</sub>)<sub>2</sub> is capable of solubilizing limited amounts of the highly hydrophobic compounds due to its short oligo(ethylene glycol) chains and thus low hydrophilic/hydrophobic ratio. Therefore, the solutions with high quantities of poorly water-soluble drugs either contain undissolved drug or coprecipitate (at a drug/LCA(EG<sub>4</sub>)<sub>2</sub> molar ratio  $\geq 0.8$  for ibuprofen,  $\geq 0.6$  for naproxen). The decrease in the mixing transition of LCA(EG<sub>4</sub>)<sub>2</sub> follows a similar trend than that of the cloud points (Figure 4b), but here the effects of acetaminophen and theophylline are negligible. Although slightly more hydrophobic than ibuprofen, naproxen has a similar effect on both  $T_{cp}$  and  $T_{mix}$  (Table 1). Hence, the mixing temperatures follow the order of the hydrophobicities of the additives.

The effect of organic additives on analogous nonionic poly(oxyethylene)-type surfactants can vary greatly depending on the compound. The short-chain water-soluble aliphatic alcohols have been reported to increase the  $T_{cp}$ , while the

sparsely water-soluble longer-chain alcohols and other hydrophobic compounds decrease it.<sup>47,48</sup> The more hydrophilic compounds remain in the solution and can favor the micelle hydration, thus increasing the cloud point.<sup>47</sup> A decrease in the cloud point has been explained by the solubilization of hydrophobes by micelles, which modifies the packing of the surfactants inducing micellar growth and/or shape change or results in the dehydration of the hydrophilic groups, depending on the site of the solubilization.<sup>47</sup> Studies on the influence of differently substituted benzaldehydes and analogous compounds on the cloud point of a well-known thermoresponsive polymer, poly(*N*-isopropylacrylamide), have suggested that not only the hydrophobicity of the additives or their effect on the solvent quality play an important role but also the direct interactions between the additive and the polymer.<sup>49,50</sup> These depend strongly on the chemical structure of the additive; for example, in the case of benzaldehydes, on the relative positions of the substituents.<sup>49</sup> Therefore, in drug carrier applications the selective interactions can result in different release kinetics for different drugs<sup>51,52</sup> and must be taken into consideration.

Here, the more hydrophilic drugs, acetaminophen and theophylline, change the solution properties of LCA(EG<sub>4</sub>)<sub>2</sub> slightly, suggesting preferential interactions with the hydrophilic domains closer to the interface with water. This is consistent with our observations on the interactions of another water-soluble drug, riboflavin ( $\log P = -1.5$ )<sup>46</sup> with oligo(ethylene glycol) derivatives of other bile acids. Lidocaine represents the case of intermediate hydrophobicity, decreasing both cloud point and mixing temperature of LCA(EG<sub>4</sub>)<sub>2</sub>, but less than the poorly water-soluble drugs, ibuprofen and naproxen. The hydrophobic compounds are expected to be solubilized by the steroid moieties of the derivative. This may perturb the molecular packing in the LCA(EG<sub>4</sub>)<sub>2</sub> self-assemblies, leading to a deteriorated quality of the gels even below the gel-to-solution temperature, while enhanced intermolecular interactions would be indicated by the increase in the transition temperature and the hardening of the gel.<sup>53</sup>

Indeed, a 14.5 wt % solution with ibuprofen/LCA(EG<sub>4</sub>)<sub>2</sub> molar ratio of 0.4 exhibits storage modulus of the range of a 5.0 wt % LCA(EG<sub>4</sub>)<sub>2</sub> solution without the added drug ( $f = 1$  Hz, data shown in Figure S2 of the Supporting Information) and, hence, poorer mechanical properties than in the absence of the drug. Here, the LCA(EG<sub>4</sub>)<sub>2</sub> concentration above the threshold concentration of  $\sim 9$  wt % was selected to better visualize the possible changes in the gel. Ibuprofen was selected with a drug/LCA(EG<sub>4</sub>)<sub>2</sub> molar ratio of 0.4 because of the clear decrease in  $T_{mix}$  with this drug as shown in Figure 4, while still maintaining a suitable temperature range for testing the viscoelastic properties without precipitation. The number of experiments was kept low to make our point due to the large amount of the sample needed for the rheology tests. The sample resembles rather the solutions of entangled wormlike micelles<sup>54,55</sup> than gels, showing viscous behavior at low oscillation frequencies ( $G'' > G'$ ) and elastic behavior at high frequencies ( $G' > G''$ ) with a crossover at the lower end of the frequency range ( $f(\text{crossover}) \sim 0.005$  Hz). Such behavior was not observed for the additive-free samples in the same concentration range. In addition, when the sample was left standing for several weeks at 5 °C, it remained cloudy, suggesting higher structural inhomogeneity or lower stability than in the absence of a drug.

The results demonstrate the strong dependence of the thermoresponsiveness of the bile acid oligo(ethylene glycol) derivatives on their hydrophilic/hydrophobic balance. This

balance can be altered by organic additives, suggesting the importance of hydrophobic interactions in the self-assembly of the molecules. Although the effects of the additives may be partially explained by their different hydrophobicities, literature examples have shown that selective interactions can have strong influence on the thermosensitive systems and thus cannot be ruled out. The pegylation of lithocholic acid not only brings about the two thermal transitions but also increases the water solubility at neutral pH and brings the gel-to-solution transition temperature closer to the body temperature, giving promise to biomedical and pharmaceutical applications.

#### 4. CONCLUSIONS

The thermoresponsive self-assembling behavior of oligo-(ethylene glycol) derivatives of bile acids depends on the number and length of the grafts and thus on the hydrophilic/hydrophobic balance of the compounds. Upon cooling below a threshold temperature, one of the derivatives, LCA(EG<sub>4</sub>)<sub>2</sub>, self-assembles to form hollow nanotubes responsible for the gelation of a concentrated solution with time. The concentration dependence of the plateau modulus shows two scaling regimes. The mobility of the nanotubes around the cross-linking points is reduced at high concentrations, arising from the ordered microdomains—bundles of nanotubes—acting as cross-links. In semidilute solutions, the strength of the gel decreases strongly upon dilution and the linkers between the aggregated domains rupture easily. The self-assembling process is perturbed by the addition of hydrophobic organic compounds, leading to a decrease in both the cloud point and the mixing temperature, and poorer mechanical properties of the gel. The results highlight the self-assembling process of LCA(EG<sub>4</sub>)<sub>2</sub> as well as its interactions with compounds of different polarities, although the site of solubilization may vary and selective interactions may be present. Hence, further studies on the self-assembling characteristics may be warranted.

#### ■ ASSOCIATED CONTENT

##### Supporting Information

WAXS pattern and the spectrum of the equilibrated 14.5 wt % aqueous solution of LCA(EG<sub>4</sub>)<sub>2</sub> and the mechanical spectrum of the solution with ibuprofen at ibuprofen/LCA(EG<sub>4</sub>)<sub>2</sub> molar ratio 0.4. This material is available free of charge via the Internet at <http://pubs.acs.org>.

#### ■ AUTHOR INFORMATION

##### Corresponding Author

\*Fax 1-514-340-5290; Tel 1-514-340-5172; e-mail [julian.zhu@umontreal.ca](mailto:julian.zhu@umontreal.ca).

##### Notes

The authors declare no competing financial interest.

#### ■ ACKNOWLEDGMENTS

NSERC of Canada, FQRNT of Quebec, and the Canada Research Chair program are acknowledged for financial support. The authors are also members of CSACS funded by FQRNT and GRSTB funded by FRSQ. The help of Drs. Jeannie Mui, S. Kelly Sears, and Hojatollah Vali at McGill University with the freeze-fracture technique and transmission electron microscopy, and that of Sylvain Essiembre at the University of Montreal with WAXS is gratefully acknowledged.

#### ■ REFERENCES

- (1) Christian, D. A.; Cai, S.; Garbuzenko, O. B.; Harada, T.; Zajac, A. L.; T. Minko, T.; Discher, D. E. *Mol. Pharmaceutics* **2009**, *6*, 1343–1352.
- (2) Shimizu, T.; Masuda, M.; Minamikawa, H. *Chem. Rev.* **2005**, *105*, 1401–1443.
- (3) Zhou, Y. *Sci. Adv. Mater.* **2010**, *2*, 359–364.
- (4) Lee, S. B.; Koepsel, R.; Stolz, D. B.; Warriner, H. E.; Russell, A. J. *J. Am. Chem. Soc.* **2004**, *126*, 13400–13405.
- (5) Wang, Z.; Medforth, C. J.; Shelnutt, J. A. *J. Am. Chem. Soc.* **2004**, *126*, 16720–16721.
- (6) Yu, L.; Banerjee, I. A.; Gao, X.; Nuraje, N.; Matsui, H. *Bioconjugate Chem.* **2005**, *16*, 1484–1487.
- (7) Shimizu, T. Self-Assembled Organic Nanotubes and Their Applications in Nano-Bio Fields. In *Molecular- and Nano-Tubes*; Hayden, O., Nielsch, K., Eds.; Springer: New York, 2011; pp 31–74.
- (8) Madenci, D.; Egelhaaf, S. U. *Curr. Opin. Colloid Interface Sci.* **2010**, *15*, 109–115.
- (9) Mukhopadhyay, S.; Maitra, U. *Curr. Sci.* **2004**, *87*, 1666–1683.
- (10) Terech, P.; Dourdain, S.; Bhat, S.; Maitra, U. *J. Phys. Chem. B* **2009**, *113*, 8252–8267.
- (11) Babu, P.; Sangeetha, N. M.; Maitra, U. *Macromol. Symp.* **2006**, *241*, 60–67.
- (12) Svobodova, H.; Noponen, V.; Kolehmainen, E.; Sievänen, E. *RSC Adv.* **2012**, *2*, 4985–5007.
- (13) Luo, J.; Chen, Y.; Zhu, X. X. *Synlett* **2007**, *14*, 2201–2204.
- (14) Luo, J.; Chen, Y.; Zhu, X. X. *Langmuir* **2009**, *25*, 10913–10917.
- (15) Zhang, J.; Luo, J.; Zhu, X. X.; Junk, M. J. N.; Hinderberger, D. *Langmuir* **2010**, *26*, 2958–2962.
- (16) Janout, V.; Regen, S. L. *Bioconjugate Chem.* **2009**, *20*, 183–192.
- (17) Luo, J.; Giguère, G.; Zhu, X. X. *Biomacromolecules* **2009**, *10*, 900–906.
- (18) Giguère, G.; Zhu, X. X. *Biomacromolecules* **2010**, *11*, 201–206.
- (19) Strandman, S.; Le Devedec, F.; Zhu, X. X. *Macromol. Rapid Commun.* **2011**, *32*, 1185–1189.
- (20) Fujimatsu, H.; Ogasawara, S.; Kuroiwa, S. *Colloid Polym. Sci.* **1988**, *266*, 594–600.
- (21) Zhao, J.; Jeromenok, J.; Weber, J.; Schlaad, H. *Macromol. Biosci.* **2012**, *12*, 1272–1278.
- (22) Danino, D.; Talmon, Y. Direct-Imaging and Freeze-Fracture Cryo-Transmission Electron Microscopy of Molecular Gels. In *Molecular Gels. Materials with Self-Assembled Fibrillar Networks*; Weiss, R., Terech, P., Eds.; Springer: Dordrecht, 2006; pp 253–274.
- (23) Nguyen, T. T. T.; Simon, F. X.; Schmutz, M.; Mésini, P. J. *Chem. Commun.* **2009**, 3457–3459.
- (24) Scanlon, S.; Aggeli, A. *Nano Today* **2008**, *3*, 22–30.
- (25) Valéry, C.; Pouget, E.; Pandit, A.; Verbavatz, J. M.; Bordes, L.; Boisdé, I.; Cherif-Cheikh, R.; Artzner, F.; Paternostre, M. *Biophys. J.* **2008**, *94*, 1782–1795.
- (26) Valéry, C.; Paternostre, M.; Robert, B.; Gulik-Krzywicki, T.; Narayanan, T.; Dedieu, J. C.; Keller, G.; Torres, M. L.; Cherif-Cheikh, R.; Calovo, P.; Artzner, F. *Proc. Natl. Acad. Sci. U. S. A.* **2003**, *100*, 10258–10262.
- (27) Terech, P.; Friol, S. *Macromol. Symp.* **2006**, *241*, 95–102.
- (28) Schefer, L.; Sanchez-Ferrer, A.; Adamcik, J.; Mezzenga, R. *Langmuir* **2012**, *28*, 5999–6005.
- (29) Terech, P.; Smith, W. G.; Weiss, R. G. *J. Chem. Soc., Faraday Trans.* **1996**, *92*, 3157–3162.
- (30) Terech, P.; Sangeetha, N. M.; Maitra, U. *J. Phys. Chem. B* **2006**, *110*, 15224–15233.
- (31) Rixman, M. A.; Dean, D.; Ortiz, C. *Langmuir* **2003**, *19*, 9357–9372.
- (32) Fuhrhop, J. H.; Wang, T. *Chem. Rev.* **2004**, *104*, 2901–2937.
- (33) Terech, P.; Friol, S.; Sangeetha, N.; Talmon, Y.; Maitra, U. *Rheol. Acta* **2006**, *45*, 435–443.
- (34) Terech, P.; Jean, B.; Ne, F. *Adv. Mater.* **2006**, *18*, 1571–1574.
- (35) Borzacchiello, A.; Ambrosio, L. Structure-Property Relationships in Hydrogels. In *Hydrogels: Biological Properties and Applications*; Barbucci, R., Ed.; Springer: Milan, 2009; pp 9–12.

- (36) Solomon, M. J.; Spicer, P. T. *Soft Matter* **2010**, *6*, 1391–1400.
- (37) Qiao, Y.; Lin, Y.; Yang, Z.; Chen, H.; Zhang, S.; Yan, Y.; Huang, J. *J. Phys. Chem. B* **2010**, *114*, 11725–11730.
- (38) Terech, P.; Pasquier, D.; Bordas, V.; Rossat, C. *Langmuir* **2000**, *16*, 4485–4494.
- (39) MacKintosh, F. C.; Käs, J.; Janmey, P. A. *Phys. Rev. Lett.* **1995**, *75*, 4425–4428.
- (40) Schmidt, F. G.; Hinner, B.; Sackmann, E.; Tang, J. X. *Phys. Rev. E* **2000**, *62*, 5509–5517.
- (41) Lin, Y. C.; Koenderink, G. H.; MacKintosh, F. C.; Weitz, D. A. *Macromolecules* **2007**, *40*, 7714–7720.
- (42) Wu, H.; Morbidelli, M. *Langmuir* **2001**, *17*, 1030–1036.
- (43) Hietala, S.; Strandman, S.; Järvi, P.; Torkkeli, M.; Jankova, K.; Hvilsted, S.; Tenhu, H. *Macromolecules* **2009**, *42*, 1726–1732.
- (44) Abdala, A. A.; Wu, W.; Olesen, K. R.; Jenkins, R. D.; Tonelli, A. E.; Khan, S. A. *J. Rheol.* **2004**, *48*, 979–994.
- (45) Valenta, C.; Nowack, E.; Bernkop-Schnürch, A. *Int. J. Pharm.* **1999**, *185*, 103–111.
- (46) Syracuse Research Corporation, Physical/Chemical Property Database (PHYSPROP). SRC Environmental Science Center, Syracuse, NY, 1994.
- (47) Diaz-Fernandez, Y.; Rodriguez-Calvo, S.; Perez-Gramatges, A. *Phys. Chem. Chem. Phys.* **2002**, *4*, 5004–5006.
- (48) Gu, T.; Galera-Gomez, P. A. *Colloids Surf., A* **1999**, *147*, 365–370.
- (49) Hofmann, C.; Schönhoff, M. *Colloid Polym. Sci.* **2009**, *287*, 1369–1379.
- (50) Dhara, D.; Chatterji, P. R. *Langmuir* **1999**, *15*, 930–935.
- (51) Coughlan, D. C.; Quilty, F. P.; Corrigan, O. I. *J. Controlled Release* **2004**, *98*, 97–114.
- (52) Coughlan, D. C.; Corrigan, O. I. *Int. J. Pharm.* **2006**, *313*, 163–174.
- (53) de Jong, J. J. D.; Feringa, B. L.; van Esch, J. Responsive molecular gels. In *Molecular Gels. Materials with Self-Assembled Fibrillar Networks*; Weiss, R. G., Terech, P., Eds.; Springer: Dordrecht, 2006; pp 895–927.
- (54) Ahmed, T.; Aramaki, K. *J. Colloid Interface Sci.* **2008**, *327*, 180–185.
- (55) Buchanan, M.; Atakhorrami, M.; Palierne, J. F.; MacKintosh, F. C.; Schmidt, C. F. *Phys. Rev. E* **2005**, *72*, 011504–011509.